

Anchoring properties of lyotropic liquid crystals near the nematic-isotropic transition

E.A. Oliveira and A.M. Figueiredo Neto

Instituto de Física, Universidade de São Paulo, Caixa Postal 20516, 01498-970 São Paulo, São Paulo, Brazil

(Received 9 June 1993; revised manuscript received 22 September 1993)

In lyotropic liquid crystals the director at the boundary surfaces can be oriented by an external magnetic field, with a time constant τ_s about 10^3 times greater than that in the bulk. Measurements of τ_s are presented for a lyotropic sample of potassium laurate, decanol, and water in the nematic calamitic phase (N_C) in the vicinity of the nematic-isotropic transition. It is shown that τ_s decreases linearly in the N_C phase when the temperature approaches T_c [Oliveira, Figueiredo Neto, and Durand, *Phys. Rev. A* **44**, 825 (1991)].

PACS number(s): 61.30.Gd, 64.70.Md, 68.45.-v

The anchoring properties of lyotropic liquid crystals started to be investigated only in the past few years [1,2] and a behavior different from thermotropics was then revealed. In lyotropics, the director at the boundary surfaces can be aligned by an external magnetic field, with a characteristic time longer than that in the bulk ($\sim 10^3$ times greater). This means that there is a gliding process of the director at the boundary surfaces.

Although the physics involved in this process has not been completely understood yet, an alternative qualitative model has been proposed [1], based on the existence of an amphiphilic bilayer at the boundary surface with defects or channels, like a lamellar order. According to this model, the defects are interpreted as large anisotropic objects which glide and align parallel to the magnetic field.

Lyotropic liquid crystals present very rich phase diagrams with both uniaxial nematic phases; discotic (N_D) and calamitic (N_C) and the biaxial nematic phase (N_{BX}) [3,4]. They are very interesting systems for studying phase transitions.

The nematic to isotropic transition is satisfactorily described by a mean-field approximation which predicts this transition to be first order and there are many experimental data to sustain it [5,6]. The transition is always accompanied by discontinuities in density, birefringence [7], etc. However, as these discontinuities are small, some authors prefer the denomination "weakly first order" [8]. Another reason for this denomination is that liquid crystals exhibit critical behavior on cooling to temperatures close to T_c (the critical temperature) what has been termed "pretransitional behavior." These effects near T_c are typical of second-order transitions, but in the case of liquid crystals, this is explained by the short-order effects that will be important at temperatures just above T_c .

Saupe and collaborators performed experiments determining some response for functions such as density, susceptibility, and electric conductivity in all nematic domains. There are some data with respect to nematic-isotropic transition which follow the mean-field behavior [9-11]. Recently, more accurate measurements [12,13] have shown deviations from the mean-field behavior for the nematic uniaxial-biaxial transition in the vicinity of

T_c . The critical exponents β and γ derived from experiments are in agreement with the theoretical values of the XY model.

In this paper, we shall extend the study of anchoring properties of a lyotropic liquid crystal in the vicinity of the nematic-isotropic transition. The lyotropic mixture is composed of potassium laurate (KL), decanol (DeOH), and water. The advantage of using this mixture is that many physical parameters are known for it [11,12,14].

We investigate the orientation process in the N_C phase, where a magnetic field is applied, measuring the transmittance of the sample. In order to fit the experimental data, we built a model of a three-layered sample with different orientation times for the bulk and the boundaries. The fitting parameter is the characteristic orientation time in the boundaries. The determination of the orientation time as function of temperature and the knowledge of the behavior of χ_a in the neighborhood of the nematic-isotropic transition allow us to discuss how an "effective rotational viscosity" depends on temperature.

I. EXPERIMENT

The lyotropic liquid crystal is composed of potassium laurate (29.4 wt. %), decanol (6.6 wt. %), and water (64 wt. %). It presents a calamitic nematic phase between two isotropic phases [3]. The transition temperatures are about 17°C and 50°C. The sample is encapsulated inside microslides (*Vitro Dynamics*) 200 μm thick and 4 mm wide.

The measurement of the birefringence is performed with the sample previously aligned, in a strong magnetic field ($H \sim 18$ kG). The sample is placed in a temperature controlled device (accuracy 0.2°C) in a polarizing microscope with a compensator. There is no applied field, during the measurements.

The experimental setup used to investigate the orientation and relaxation process is illustrated in Fig. 1. A rotatory stage is placed between the poles of an electromagnet. The sample is placed in a temperature controlled device (accuracy 0.2°C) which is attached to the rotatory stage. The laboratory frame axes are defined with the x axis parallel to the magnetic field \mathbf{H} and z perpen-

dicular to the plane of the rotatory stage. The sample is initially uniformly oriented by a strong magnetic field (~ 18 kG) with the director parallel to the length of the microslide. Therefore (with $H = 0$), the sample is rotated from 45° in the xy plane and a magnetic field \mathbf{H} is applied. The orientation process is studied by measuring the intensity of the transmitted light, by means of a photodetector, which is coupled to a microcomputer. The same measurements are made during the relaxation process when \mathbf{H} is switched off.

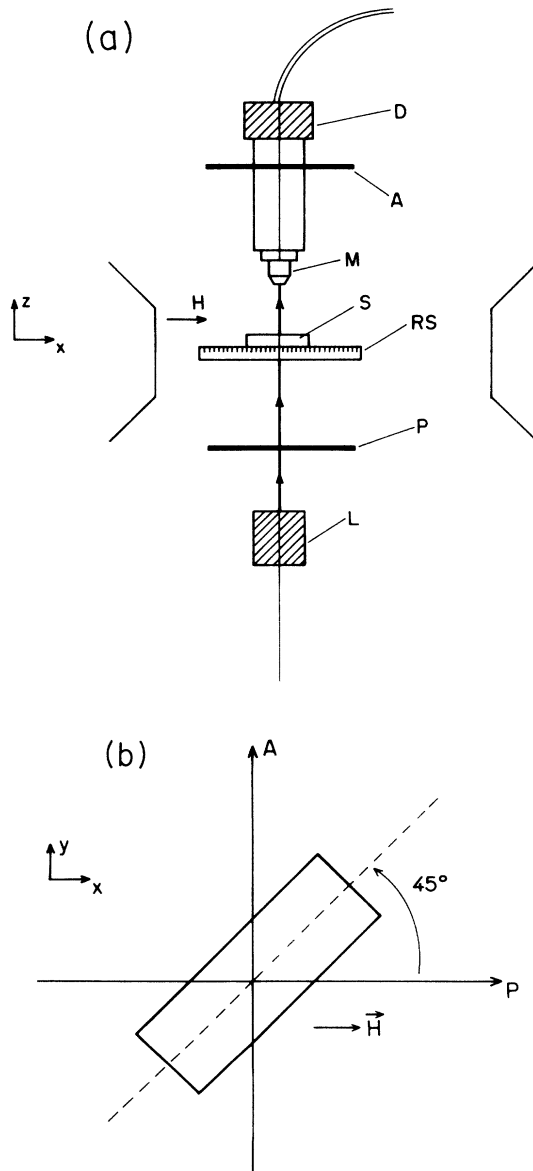


FIG. 1. Experimental setup to study orientation and relaxation process. (a) L = light source, P = polarizer, RS = rotatory stage, S = sample, M = microscope objective, A = analyzer, D = detector. (b) Top view of experimental setup showing the orientation of polarizer and analyzer relative to the sample during the orientation process. At $t = 0$ \mathbf{n} is parallel to the length of the microslide and $H = 0$.

II. THEORY

A. Orientation process ($H \neq 0$)

The dynamics of orientation of nematic liquid crystal films in a magnetic field was first studied by Brochard, Pieranski, and Guyon [15,16]. They proposed a solution to the balance of torques equation in the limit of small distortions ($H > H_c$) and strong anchoring at the boundaries ($\theta = 0$ for $z = 0$ and $z = d$). The distortion along the thickness will be

$$\theta = \theta_m(t) \sin \frac{\pi z}{d}, \quad (1)$$

where θ is the angle between the easy axis and the director \mathbf{n} and θ_m is the maximum distortion angle. For large values of t a stationary state is reached, with a time constant $S_0^{-1}(H)$ [16]

$$S_0(H) = \frac{\chi_a H_c^2}{\gamma_1} \left[\frac{H^2}{H_c^2} - 1 \right], \quad (2)$$

where χ_a is the anisotropic magnetic susceptibility and $H_c = (\pi/d)(K/\chi_a)^{1/2}$. The thickness of the slab is d , K is the elastic constant, and γ_1 is the rotational viscosity.

For large magnetic fields, the equilibrium state will correspond to the director aligned parallel to H , in the most of the slab, except for two thin transition regions of thickness ξ [$\xi = (K/\chi_a)^{1/2}/H$] near each boundary surface. When $H \gg H_c$, the time constant is expected to be proportional to H^{-2} (see also Ref. [5], p. 175). Therefore, this orientation process is only concerned to the bulk, provided that a strong anchoring at the boundaries was assumed [$\theta(0, t) = \theta(d, t) = 0$].

In lyotropics, the orientation of the director in the bulk is also observed [1,11] and the results derived by Pieranski remain valid. Typical values of S_0^{-1} for lyotropics are about 10 s. However, besides this bulk orientation, there is also a slower orientation at the boundaries. This can be explained by a simple model.

We assume that the director is uniformly oriented parallel to \mathbf{H} , except in the thin boundary layers of thickness ξ , and that there is a bilayer of amphiphilic molecules at the boundary surface like a lamellar structure. There are defects in the bilayer structure like channels [17,18] or holes. The amphiphilic medium behaves like islands surrounded by water. In this picture, the amphiphilic islands (AI) can be interpreted as large anisotropic objects, which can glide and orient parallel to an external magnetic field. There is a competition between the initial orientation in the thin boundary layer and the orientation of the bulk, imposed by the magnetic field. If the surface dimensions of the AI are comparable to ξ , they glide and orient parallel to \mathbf{H} . The dynamical equilibrium is expressed by the balance of the elastic and viscous torques.

To rotate an object with dimensions L and ℓ in the x - y plane and thickness d , one must exert a torque $\mathcal{T} = \gamma_1 \theta \ell L d$. The total number of objects or AI is $\alpha S \xi / d$, where α is the number of AI per unit area and S is the boundary surface area. Therefore, the torque per unit

area is $\mathcal{T} = \gamma_1 \theta \xi \alpha$. The balance of the torque at the surface is written as

$$\gamma_1 \dot{\theta} \xi \alpha \cong \frac{K}{\xi} (\theta_{\max} - \theta), \quad (3)$$

where θ_{\max} is the maximum angle distortion in the bulk. The solution of this equation gives an exponential increasing of θ , with a time constant τ_s :

$$\tau_s = \frac{\xi^2 \gamma_1 \alpha}{K} = \frac{\gamma_1 \alpha}{\chi_a H^2}. \quad (4)$$

If the dimensions of the AI are about ξ , and ξ is about $20 \mu m$, for $H = 4$ kG, the parameter α can be estimated to the order of 10^4 , if the AI occupy half of the surface.

B. Relaxation process

When the magnetic field is switched off before the relaxation process has been completed, the distortion in the bulk relaxes as if there was a strong anchoring at the boundary surfaces. The final orientation will be almost uniform and parallel to the orientation of the surface boundary layers.

There is also a relaxation process in the boundary layers. Different orientations of the AI in these layers result in an elastic torque. Let us call θ the angle between the axis of two-neighbor AI. The viscous torque per unit area will be $\mathcal{T} = \gamma_1 \theta \ell \alpha$, which is equal to the elastic torque. The balance of torques equation is written as

$$\gamma_1 \alpha \dot{\theta} \ell = \frac{K}{\xi} \theta. \quad (5)$$

As ℓ is comparable to ξ and $\alpha = (1 \text{ cm}^2 / \ell L)$, the characteristic relaxation time will be

$$\tau_r \cong \gamma_1 / K. \quad (6)$$

With typical values of γ_1 and K for lyotropic liquid crystals we obtain $\tau_r \sim 10^5$ s.

C. The transmittance of the sample

The transmittance of the sample can be calculated by considering the nonuniform anisotropic medium as consisting of many thin layers and treating each layer as homogeneous, with uniform orientation. If one supposes that the sample with thickness d is broken up into m layers, the orientation of each layer will be given by θ , relative to a reference frame axes. We also assume that the incident light is linearly polarized and the incidence is normal to the layer. In each layer, the incident electric field is decomposed in two components parallel and perpendicular to the director and a phase difference is also introduced. The calculations are simplified using Jones matrix (Appendix A).

We calculate the transmittance of the sample considering two possible configurations of the director: the first one described by a sine wave and the second one

described by the three-layered sample model *presented above*.

In the first case, we assume that the distortion has a sine-wave shape, similar to Eq. (1). However, we shall remove the constraints at the surface. The orientation of the director at the surface will be given by θ_s :

$$\theta_s(t) = \theta_m (1 - e^{-t/\tau_s}). \quad (7)$$

The amplitude of the sine wave is variable, and written as

$$\theta(z, t) = (\theta_m - \theta_s(t)) \text{sen} \frac{\pi z}{d}. \quad (8)$$

The equilibrium corresponds to a uniform orientation with the director parallel to the magnetic field.

In the second configuration, the sample is broken up in only three layers. The thickness of the boundary layers is ξ and the orientation is given by $\theta_s(t)$. The director orients, in the bulk, parallel to \mathbf{H} , with a time constant $\tau_o(H)$.

Making use of the experimental setup shown in Fig. 1, it is expected that the intensity of the transmitted light is maximum for $t = 0$, when \mathbf{H} is turned on and will decrease with the time ($H > 0$). The maximum distortion angle θ_m will be $\pi/4$. Values of the viscosity and susceptibility are reported in the literature [19–21] and τ_v is known. The values of τ_s can be calculated except for the factor α . This factor will be used as the fitting parameter to the experimental results.

III. RESULTS AND DISCUSSION

A. Determination of T_c

The anisotropic optical susceptibility $\overset{\leftrightarrow}{\epsilon}$ is a good choice for the order parameter in lyotropics, which is expressed as a function of the birefringence Δn [7]. In the mean-field theory, the free energy is expanded in terms of the invariants of the order parameter. We shall be particularly interested in the invariant σ_3 defined as

$$\sigma_3 = 4\epsilon_1 \epsilon_2 \epsilon_3, \quad (9)$$

where ϵ_i ($i = 1, 2, 3$) are the diagonal elements of the traceless tensor $\overset{\leftrightarrow}{\epsilon}$. The mean-field theory predicts that σ_3 depends linearly on the temperature T in the nematic phases. In this picture σ_3 is proportional to $(\Delta n)^3$, which can be experimentally determined. The results obtained for the sample used in this investigation is shown in Fig. 2. It is seen in Fig. 2(a) that the order parameter decreases near the transition to the isotropic phase. The transition temperature T_c is obtained from Fig. 2(b) plotting σ_3 as a function of temperature. The solid line in Fig. 2(b) corresponds to a linear fitting of the experimental data. When $\sigma_3 = 0$, we obtain $T_c = 50.51^\circ \text{C}$.

B. Orientation process ($H \neq 0$)

We measure the transmittance of a initially uniform oriented sample, when a magnetic field \mathbf{H} is applied at

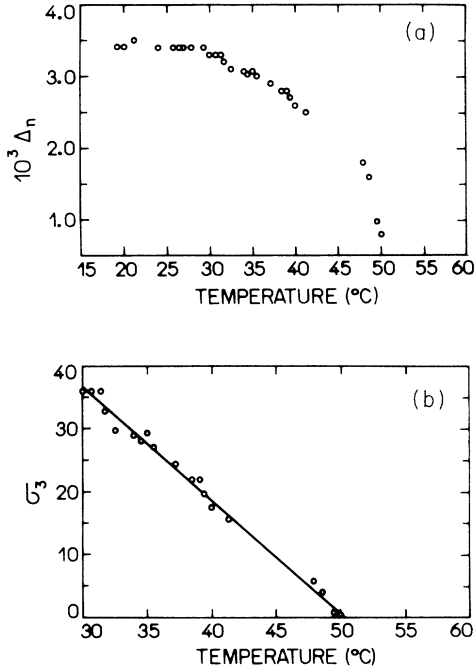


FIG. 2. (a) Birefringence as a function of the temperature. (b) Invariant of the order parameter σ_3 as a function of the temperature.

45° from the initial orientation. Typical experimental curves are shown in Fig. 3(a) corresponding to the transmittance of the sample as a function of the time, for different intensities of the magnetic field. There is a comparison between the calculated transmittance of the sample for the two configurations *discussed above* and the experimental results in Fig. 3(b). The curve corresponding to the sine wave configuration was obtained dividing the sample in 50 layers. The shape of the curve does not change with a greater number of layers. By means of this configuration, it is not possible indeed to find a value of α that fits well the experimental data. It is clear from this picture that the model of three layers represents a good approximation to the configuration of the director.

The values of α and τ_s obtained are listed in Table I, for different values of H . The value of α is almost constant and the average is $\bar{\alpha} = 940$. The listed values of τ_s for $H = 7$ and 14 kG were determined by applying the magnetic field at 5° from the initial orientation, but the surface orientation time does not depend on this angle. The experimental values of τ_s depend on H , as it is outlined in a log-log plot; see Fig. 4. The exponent of H derived from the log-log plot, is -1.96 ± 0.20 . The uncertainty in τ_s is about 8%. This behavior is compatible with what is expected from Eq. (4).

C. Temperature effects in τ_s

The surface orientation process depends on temperature, as it is shown in Table II, for $H = 8$ kG. We must remark that when temperature increases, at about 4°C below T_c , the fitting to the experimental curves of transmittance using the model of a three-layered sam-

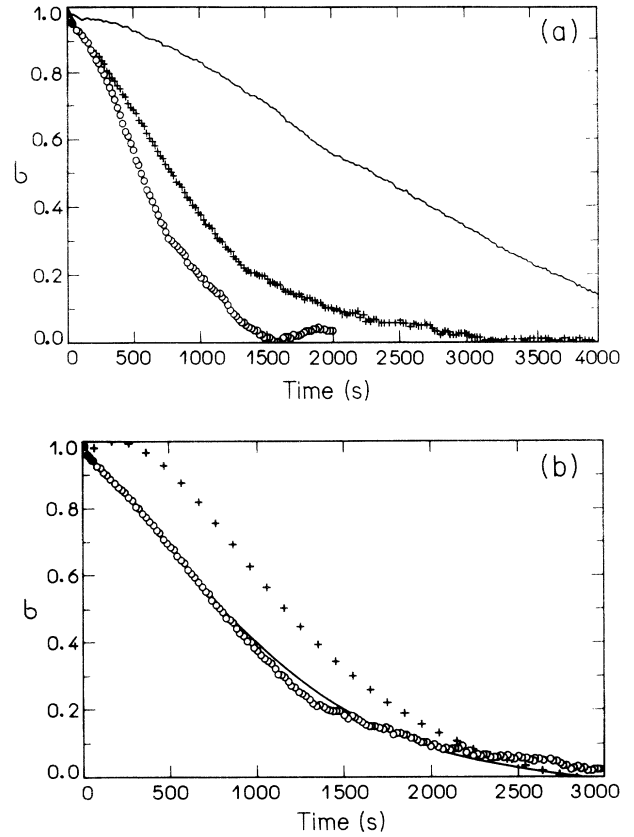


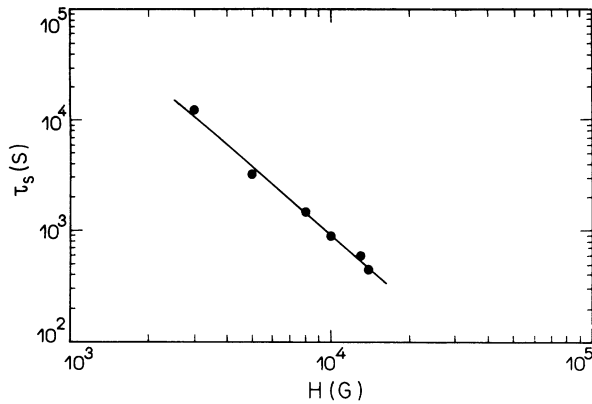
FIG. 3. (a) Intensity of the transmitted light as a function of the time for $H = (-) 5$ kG, $(+) 8$ kG, and $(\bullet) 10$ kG. (b) Calculated transmittance for the $(-)$ sine wave and $(+)$ three layers model with $H = 8$ kG. In both cases $\alpha = 950$.

ple with the boundary layers of thickness ξ is very poor. The sine-wave configuration also fails in this fitting. The best fitting is obtained, assuming that the configuration of the director is described by a three-layered sample of equal thickness. A possible explanation for that would be given if the order imposed by the boundary surface layer propagates through a length larger than ξ .

We notice that τ_s decreases when the temperature approaches T_c . The dependence of τ_s on temperature is obtained from a log-log plot (Fig. 5). The decreasing of τ_s is roughly linear with temperature; $\tau_s \approx (T_c - T)$. Since τ_s combines various parameters (γ_1 , α , and χ_a)

TABLE I. Experimental values of τ_s for different values of the magnetic field H . The second column corresponds to the sample temperature during the experiment. The uncertainty in τ_s is about 8%.

H (kG)	Temperature ($^\circ\text{C}$)	α	$10^3 \tau_s$ (s)
3	28.3	1100	12.2
5	27.5	800	3.2
7	28.2	900	3.3
8	27.9	900	1.5
10	28.3	950	0.9
13	28.2	1000	0.6
14	28.1	924	0.5

FIG. 4. Dependence of τ_s on H in a log-log plot.

which also depend on temperature, if we know the way χ_a behaves near the nematic-isotropic transition, we are able to evaluate the way $\gamma_1\alpha$ behaves, as well.

Saupe and Stefanov [9] measured χ_a for a lyotropic sample of decylammonium chloride, ammonium chloride, and water. These mixtures present a lamellar, a nematic (discotic), and an isotropic phase. They observed that χ_a decreases in the nematic range when the temperature (T) approaches the transition to the isotropic phase. The decreasing of χ_a is linear on T , within a range of 15 °C below T_c . There is also a two-phase region beginning at 2 °C below T_c and a discontinuity of χ_a , typical of a first-order transition [9].

In our experiment, we measure τ_s in the nematic phase as a function of temperature, in a range of ~ 20 °C below the transition to the isotropic phase. If we assume that χ_a behaves in the same way described by Saupe, we are able to evaluate the way that the product $\gamma_1\alpha$ behaves, as well. We should say that $\tau_s \approx (T_c - T)$ (Fig. 5) and $\chi_a \approx (T_c - T)$ (from Ref. [9] measurements). Therefore, from Eq. (4), we obtain

$$\gamma_1\alpha \approx (T_c - T)^2. \quad (10)$$

We may relate the decreasing of $\gamma_1\alpha$ when T approaches T_c to a decreasing of the area occupied by the amphiphilic islands at the boundary layers. Actually, we can refer to $\gamma_1\alpha$ as an *effective rotational viscosity* at the boundary layers.

TABLE II. Experimental values of τ_s for $H = 8\text{ kG}$ at various temperatures.

$ T - T_c $ (°C)	$10^3 \tau_s$ (s)
1.9	133
3.0	94
4.0	250
7.2	312
9.8	422
14.7	890
16.2	1234
17.2	859
19.0	1406
22.6	1406

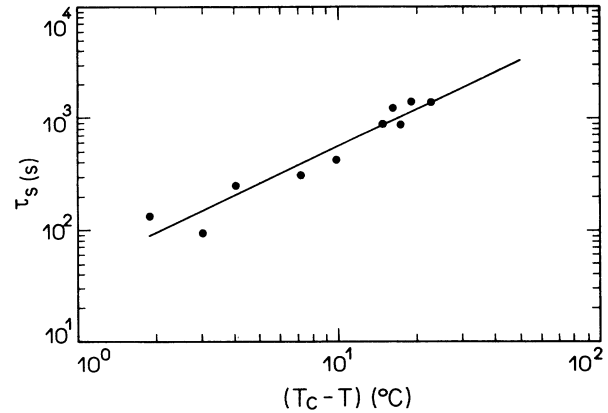


FIG. 5. Dependence of the surface orientation times on temperature.

D. Relaxation process ($H = 0$)

When the magnetic field H is switched off before the orientation process has been completed, we are able to observe that the transmittance of the sample decreases very slowly.

According to the proposed model, this slow relaxation process is related to small variations of θ_s in the surface boundary layers. The transmittance can be calculated admitting a uniform sample oriented along θ_s . When θ_s is small, the transmittance is proportional to θ_s^2 . If θ_s decreases with a time constant τ_r , the transmittance decreases with a time constant $\tau' = \tau_r/2$.

In Fig. 6 an exponential curve is fitted to typical experimental curves of transmittance in the relaxation process. The values of τ_r obtained for different values of H are listed in Table III. Within our experimental error we obtain $10^4 \text{ s} < \tau_r < 4 \times 10^4 \text{ s}$. This value is smaller than the estimated value from Eq. (6). This estimation was based on values of viscosity (γ_1) elastic constant (K) reported in the literature for similar nematic mixtures. However, as we are dealing with surface processes, these values may be different, due to the order imposed by the

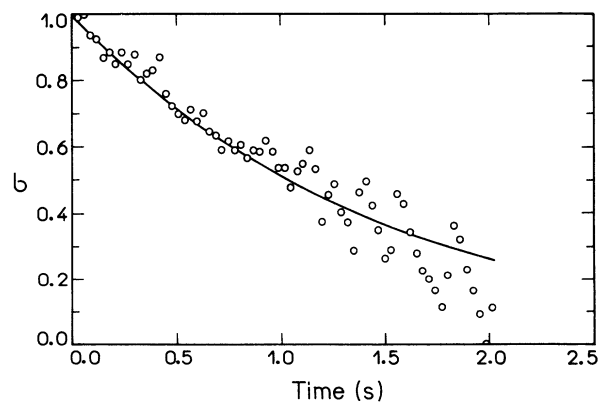
FIG. 6. Relaxation process. The solid line represents a fitting to the experimental curve of transmittance for a sample after 80 s in $H = 8 \text{ kG}$.

TABLE III. Experimental values of the relaxation time, τ_r . Δt corresponds to the time interval with H turned on.

H (kG)	Δt (s)	$10^3 \tau_r$ (s)
4	400	8
8	80	44
10	60	11
13	60	13

boundary surface. We could expect the elastic constant to be greater in the boundary layers than in the bulk. This could explain the results obtained.

IV. CONCLUSIONS

The orientation process of lyotropic liquid crystals are quite different from thermotropics. The director at the boundary surface is allowed to glide and orient parallel to the applied magnetic field. The measurements of the transmittance of the sample were shown to be a good technique to study surface processes.

In order to explain the gliding phenomenon, a model is proposed based on the existence of a bilayer at the boundaries, with defects, like in a lamellar structure. Within the accuracy of our experiment we observe that the area occupied by the amphiphilic aggregates does not depend on H . The characteristic orientation time at the boundary layer is about 10^3 times greater than the bulk orientation time and depends on H^{-2} as predicted by the gliding model. It is also observed that the configuration of the director corresponds to an almost uniform oriented sample parallel to H , except in the thin boundary layers.

A slow relaxation process is observed, which is related to the boundary layers. The characteristic time of this process is about 10^4 s and it is due to the torques between the amphiphilic islands with different orientations at the boundary layers.

The experiment shows that the characteristic surface orientation time τ_s in the nematic phase decreases, when the temperature (T) approaches the transition to the isotropic phase. The decreasing of τ_s is linear within a range of 20°C below T_c . In the nematic domain, we also expect that χ_a decreases with temperature when T approaches T_c , with a discontinuity at T_c , typical of a first-order transition. We expect indeed that $\gamma_1\alpha$ decreases when T approaches T_c , however, faster than the decreasing of τ_s and χ_a . The product $\gamma_1\alpha$, which can be interpreted as an *effective rotational viscosity* at the boundary layers, should be proportional to $(T_c - T)^2$. The decreasing of $\gamma_1\alpha$ would be related to a decreasing of the area occupied by the amphiphilic island at the boundary layers, when temperature is increased to T_c .

Within the accuracy of our experiment, we have not observed any discontinuity of τ_s at T_c . Future experiments with more precise measurements and a better resolution in temperature are necessary in order to elucidate this point.

ACKNOWLEDGMENTS

We are thankful to FAPESP for financial support.

APPENDIX A

Let us consider an anisotropic medium which will be broken up into m thin layers with uniform orientation. The thickness of each layer is θ_j and the orientation on the director is given by ζ_j ($j = 1, \dots, m$) measured from the x axis [Fig. 1(a)]. The angle between the polarized incident beam is φ . In the first layer the incident electric field \mathbf{E} is divided in two components, parallel (E_{1P}) and perpendicular to the director (E_{1T}),

$$E_{1P} = |\mathbf{E}| \cos \alpha, \quad (\text{A1})$$

$$E_{1T} = |\mathbf{E}| \sin \alpha,$$

where $\alpha = \varphi - \theta_1$.

If the birefringence of the uniform orientation layer in Δn and λ is the light wavelength, the phase difference introduced by each layer is

$$\xi_j = \frac{2\pi}{\lambda} \Delta n \zeta_j. \quad (\text{A2})$$

The components of the electric field incident in the second layer, in matrix notation, is given by

$$\begin{pmatrix} E'_{P1} \\ E'_{T1} \end{pmatrix} = D_1 \begin{pmatrix} E_{1P} \\ E_{1T} \end{pmatrix}, \quad (\text{A3})$$

where D_1 is a matrix representing the phase difference introduced by the first layer:

$$D_1 = \begin{pmatrix} 1 & 0 \\ 0 & e^{i\delta_1} \end{pmatrix}. \quad (\text{A4})$$

In the second layer, there will be a rotation of the plane of polarization, which can be represented by the matrix

$$R_2 = \begin{pmatrix} \cos \beta_2 & \sin \beta_2 \\ -\sin \beta_2 & \cos \beta_2 \end{pmatrix}, \quad (\text{A5})$$

where $\beta_2 = \theta_2 - \theta_1$.

The new components of the electric field will be

$$\begin{pmatrix} E_{P2} \\ E_{T2} \end{pmatrix} = R_2 \begin{pmatrix} E'_{P1} \\ E'_{T1} \end{pmatrix}. \quad (\text{A6})$$

Generalizing, in each layer there is a rotation of the plane of polarization and a phase difference. The rotation operation is given by the matrix R , where β_j will be

$$\beta_j = \theta_j - \theta_{j-1}. \quad (\text{A7})$$

The operation of introducing the phase difference δ_i will be effected by the matrix D_i .

These operations are repeated up to the last layer, m . Therefore, only the components of electric field parallel to A will be transmitted. The amplitude of electric field transmitted will be

$$E_{PA} = E_{Tm} \cos \beta_{m+1} - E_{Pm} \sin \beta_{m+1}, \quad (\text{A8})$$

where $\beta_{m+1} = \varphi - \theta_m$.

The intensity of the transmitted light is written as

$$I = E_{PA} E_{PA}^*. \quad (\text{A9})$$

The transmittance will be $\sigma = (I_{\max} - I)/I_{\max}$.

- [1] E.A. Oliveira, A.M. Figueiredo Neto, and G. Durand, *Phys. Rev. A* **44**, R825 (1991).
- [2] E.A. Oliveira, P.J. Photinos, and A.M. Figueiredo Neto, *Liq. Cryst.* **14**, 837 (1993).
- [3] L.J. Yu and A. Saupe, *Phys. Rev. Lett.* **45**, 1000 (1980).
- [4] A.M. Figueiredo Neto, L. Lielert, and Y. Galerne, *J. Phys. Chem.* **89**, 3737 (1985).
- [5] P.G. de Gennes, *The Physics of Liquid Crystals* (Clarendon, Oxford, 1974), p. 48.
- [6] E.B. Priestley, P.J. Wojtowicz, and P. Sheng, *Introduction to Liquid Crystals*, edited by E.B. Priestley, (Plenum, New York, 1974), p. 41.
- [7] Y. Galerne and J.P. Marcerou, *Phys. Rev. Lett.* **51**, 2109 (1983); *J. Phys. (Paris)* **46**, 81 (1985).
- [8] This remark is considered incorrect by Peter J. Wojtowicz; see discussion, E.B. Priestley, P.J. Wojtowicz, and P. Sheng, *Introduction to Liquid Crystals* (Ref. [6]), p. 41.
- [9] M. Stefanov and A. Saupe, *Mol. Cryst. Liq. Cryst.* **108**, 309 (1984).
- [10] P.J. Photinos and A. Saupe, *J. Chem. Phys.* **84**, 517 (1986).
- [11] P. Photinos, G. Melnik, and A. Saupe, *J. Chem. Phys.* **84**, 6928 (1986).
- [12] G. Melnik, P.J. Photinos, and A. Saupe, *J. Chem. Phys.* **88**, 4046 (1988).
- [13] Z.A. de Santana and A.M. Figueiredo Neto, *Phys. Rev. A* **46**, 7630 (1992).
- [14] T. Kroin and A.M. Figueiredo Neto, *Phys. Rev. A* **36**, 2987 (1987).
- [15] F. Brochard, P. Pieranski, and E. Guyon, *Phys. Rev. Lett.* **28**, 1681 (1972).
- [16] P. Pieranski, F. Brochard, and E. Guyon, *J. Phys. (Paris)* **33**, 681 (1972); *ibid.* **34**, 35 (1972).
- [17] M.C. Holmes and J. Charvolin, *J. Phys. Chem.* **88**, 810 (1984).
- [18] J. Charvolin and Y. Hendrikx, *J. Phys. (Paris) Lett.* **41**, L597 (1980).
- [19] E. Zhou, M. Stefanov, and A. Saupe, *J. Chem. Phys.* **88**, 5137 (1988).
- [20] A. Saupe, *Nuovo Cimento* **30**, 16 (1984).
- [21] S. Plumley, Y.K. Zhu, Y.W. Hui, and A. Saupe, *Mol. Cryst. Liq. Cryst.*, **182B**, 215 (1990).